Damage monitoring in fracture mechanics by evaluation of the heat dissipated in the cyclic plastic zone ahead of the crack tip with thermal measurements

D. Palumbo, Rosa de Finis, F. Ancona, U. Galietti

Engineering Fracture Mechanics 181 (2017) 65–76

Contents lists available at ScienceDirect

Engineering Fracture Mechanics

journal homepage: www.elsevier.com/locate/engfracmech

Damage monitoring in fracture mechanics by evaluation of the heat dissipated in the cyclic plastic zone ahead of the crack tip with thermal measurements

D. Palumbo *, R. De Finis, F. Ancona, U. Galietti

Department of Mechanics, Mathematics and Management (DMMM), Politecnico di Bari, Viale Japigia 182, 70126 Bari, Italy

ARTICLE INFO

Article history:
Received 13 April 2017
Received in revised form 16 June 2017
Accepted 22 June 2017
Available online 23 June 2017

Keywords:
Martensitic steel
Heat dissipated
Crack growth
Thermography

ABSTRACT

Dissipated energy ahead of the crack tip represents a useful tool to study the fatigue crack growth. In this regard, different analytical and numerical models were proposed in literature to investigate the role of dissipated energy in fracture mechanics and experimental techniques were used to validate them. The experimental measurement of dissipated energy requires an accurate equipment and suitable techniques that may restrict the applications only to laboratory tests.

In this work, an experimental approach by using the thermographic technique has been used to assess the heat dissipated at the crack tip in the cyclic plastic zone. The proposed approach is based on the evaluation of the heat source that occurs at the twice of the loading frequency directly related to the plastic phenomena around the crack tip. This index showed to be more suitable for on field measurement. By monitoring the fatigue crack growth during a fracture mechanics test carried out on the martensitic steel AISI 422, a similar Paris Law model was obtained between the crack growth and the heat dissipated per cycle. Moreover, it was obtained a fourth power dependence of heat dissipated energy and Stress Intensity Factor (SIF) in agreement with numerical and analytical models present in literature.

1. Introduction

Material fatigue behaviour in presence of crack depends on several factors related to the material and it is governed by different micro-mechanisms of damage at the crack tip. The first approach for describing the crack growth behaviour was proposed by Paris and Erdogan [1]. In their work the crack growth rate is expressed as a function of the stress intensity factor (SIF), [2]. In this regard, the constants of Paris's Law can be obtained by use of conventional methods according to Standards [3], by means of experimental and non-destructive techniques [4–18].

In the last years, many works [19–23] have focused their attention to the energy dissipated at the crack tip and to a possible relation with the growth of cracks. The energy based approach, proposed firstly by Weertman [19], links the crack growth rate with the critical energy to create a unit surface area. Moreover, this approach predicts a fourth power dependence of the crack growth rate and Stress Intensity Factor (SIF). Similar results were obtained by Klingbeil [20], where the crack growth in ductile solids is governed by the total cyclic plastic dissipation ahead of the crack. In [21] Mazari

* Corresponding author.
E-mail address: davide.palumbo@poliba.it (D. Palumbo).

http://dx.doi.org/10.1016/j.engfracmech.2017.06.017
0013-7944/

et al. starting from the Weertman's and Klingbeil's approach, developed a new model in which a similar Paris Law model was obtained between the crack growth and the heat dissipated per cycle.

The Dimensional Analysis approach was used in [22] to describe the fatigue crack growth rate as function of an energy parameter through a similar Paris-like model.

The experimental approaches used in literature aimed to determine the critical energy (U_c) were based on the use of strain gages in the plastic zone [23,24], calorimetric measurements [25], and hysteresis loop evaluation [21]. However, these approaches require an off-line measurement and processing of data with consequent high testing time and cannot be applied on actual structural components.

Infrared Thermography (IRT) is a full-field contactless technique used in many fields such as, non-destructive testing (NDT), process monitoring and evaluation of heat sources during fatigue tests. This technique was already proposed for the study of the fracture behaviour of materials subjected to fatigue loading [11–18]. In particular, a temperature rise due to the heat dissipations can be observed around the crack tip where the plastic zone is located. In this regard, Carrascal et al. [8] used IRT for evaluating the Paris Law constants of a polymer (polyamide) with an experimental methodology. A good agreement was found with respect to traditional calculation methods. Cui et al. [9], applied IRT to study the fatigue crack growth of magnesium alloy joints and demonstrated the potential of IRT in predicting the threshold value for unstable crack growth.

In the work of Meneghetti et al. [26], experimental tests were performed for evaluating the specific heat energy per cycle averaged in a small volume surrounding the crack tip from temperature measurements.

The above exposed procedures may find limitation in those cases in which temperature changes on material related to the plastic zone are very low (short cracks) and, moreover, high performance equipment and a difficult set-up are required. This is the case, for instance, with brittle materials (such as martensitic steels), welded joints and aluminum alloys [27–29].

Interesting results in assessment of plastic zone and SIF were obtained by using the Thermoelastic Stress Analysis (TSA) [30–37]. By knowing the sum of the principal stresses, it is possible to determine the stress intensity factor and, at the same time, it is possible to determine the crack growth rate by analyzing the phase data. In this regard, Ancona et al. [38] proposed an automatic procedure based on TSA, to assess the Paris Law constants and to study the fracture behaviour of 4 stainless steels.

The aim of the work is to put the basis for a residual life estimation of a component in service conditions with a full field, contactless experimental technique able to determine the crack tip position and assess the dissipated energy per cycle. In this work, in particular, it will be presented the algorithm able to estimate the dissipated energy and define the crack tip position. Paris curve form thermographic data will allow a residual life estimation once the material is characterized.

Three CT steel (AISI 422) specimens were used and tested according to ASTM E 647-00 and the monitoring of crack tip growth was performed in a continuous manner by means of a cooled IR camera. Thermal data were processed in the frequency domain in order to extract the heat source related to the heat dissipated at the crack tip. Then, a simple method was used for estimating the heat energy dissipated per cycle. A similar Paris Law model was obtained between the crack growth and the heat dissipated per cycle. Moreover, it was obtained a fourth power dependence of heat dissipated energy and Stress Intensity Factor (SIF) in agreement with numerical and analytical models present in literature.

The proposed approach seems very promising for the on-line monitoring of crack growth during testing through a set-up which is simple compared to other techniques. Moreover, a simple specimen preparation is required, which makes the proposed procedure also suitable for the monitoring of actual structural components.

2. Theory

The heat dissipated per cycle surrounding the crack tip was evaluated taking into account a theoretical model proposed in [39]. It can be noticed in Fig. 1, that a control volume V contains the plastic area A_p of radius r_p around the crack tip. In order to deal with a detailed analysis of all the effects affecting the material behaviour, it is possible to write the first law of thermodynamics, in the well-known form to describe such phenomena:

$$W_p = \Delta U + Q \tag{1}$$

where W_p represents the mechanical energy per cycle, ΔU is the internal energy due to microstructural rearrangements, to the formation of persistent slip bands and to all the phenomena related to irreversible dislocation movements. A portion of this energy does not remain under the mechanical form but switches into heating, in particular, it contributes to the irreversible heat sources development in the material and then, affects the temperature growth [40]. Q represents the heat exchanged by convection, conduction and radiation that in a steady-state condition will correspond at the heat generated per cycle by the body during the fatigue test. All quantities are expressed in unit of volume of material.

To highlight the different energy contributions affecting the material undergoing fatigue loading (with particular regard to the energy rising in the material), the Eq. (1) can be split in several terms:

$$W_p = \oint \sigma_{ij} d\varepsilon_{ij} = \Delta U + Q = Q + E_p + E_d \tag{2}$$

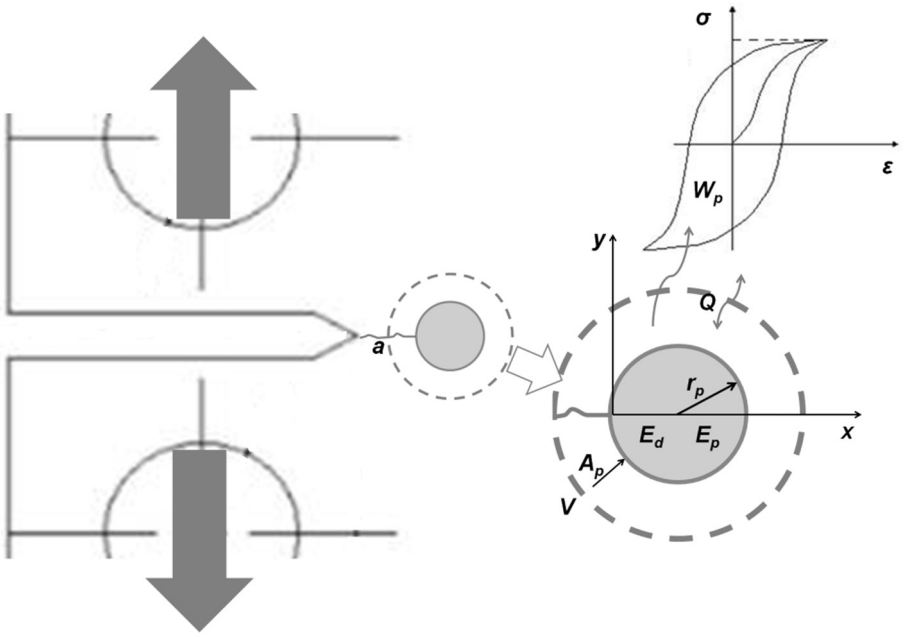

Fig. 1. Energy contributions in the plastic zone at the crack tip during a fatigue test.

The term E_p refers to the mechanical work due to plastic phenomena, that is the portion of internal energy which, as said before, is used to deform and to change irreversibly the shape of the material. The last term, at the right end of Eq. (2) (E_d), represents the energy per cycle dissipated as heat, related to plastic or viscous phenomena. This term is proportional to the total energy dissipated at the crack tip and it is used in this work to investigate the crack growth behaviour.

Just to model the phenomenon, by referring to the plastic volume in correspondence of the cyclic plastic zone (A_p area), let us consider a simplified bilinear model of the hysteresis loop, Fig. 2(a), which disregards the kinematic and isotropic hardening phenomena (stress-strain curve of elastoplastic perfectly-plastic material). In presence of a linear elastic behaviour of material (tract *a*-*b*), all the elastic energy is recovered in one cycle by the material and no irreversible dissipative sources are generated. When plastic phenomena occur, part of the total mechanical energy is dissipated as heat two times in one cycle during both the tensile loading (*a*-*b*) and the compression loading (*c*-*d*).

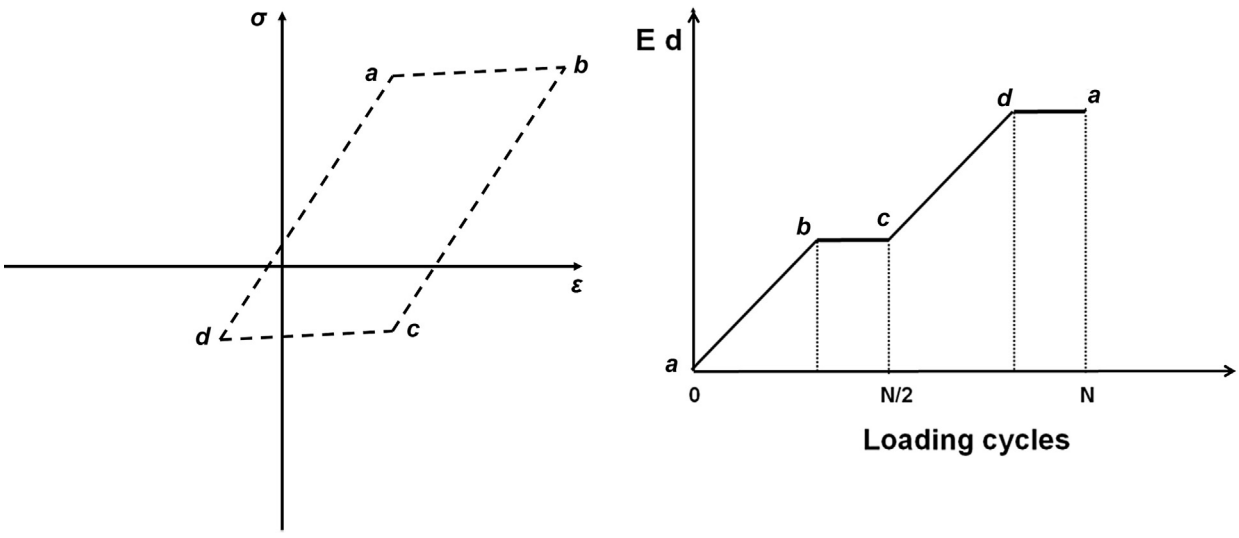

Fig. 2. (a) Bilinear model of a generic hysteresis loop and (b) trend of the heat dissipated energy E_d in a unit volume of material in a loading cycle.

Under the hypothesis:

- that most of the dissipated energy is converted to heat,
- adiabatic conditions ($Q = 0$),
- that the heat dissipated energy in the material increases linearly from a to b, and c to d points of diagram [41],

the heat dissipated energy E_d in a unit volume of material can be assumed increasing linearly during a loading cycle described by a bilinear constitutive equation, as represented in Fig. 2(b). As consequence of this, temperature in the plastic zone increases as the number of cycles increases. However, in presence of heat exchanges ($Q \neq 0$), the temperature increases until a steady state value is reached, [39].

In next sections, it will be shown the experimental set-up and methods used for evaluating the heat dissipated per cycles and then, the crack growth rate during the fatigue tests.

3. Experimental set-up

3.1. Specimen geometry and materials

The tested material is the martensitic steel AISI 422. The percentage of chromium is 11–13% in weight, and moreover, the presence of W, V and Mo alloys in the lattice, favorites the complex carbide precipitation. So, this steel can be tempered at relative high temperature (650 °C) without having chromium depleting of the lattice.

In Tables 1 and 2 are presented its chemical composition and the mechanical properties [42].

Three Compact Tension (CT) specimens were used with dimensions according to ASTM E 647 [3]. In Fig. 3, dimensions of the specimen are reported in mm. Specimens were sprayed with flat black spray for increasing the emissivity to 0.95.

3.2. Testing procedure

The tests were carried out with the MTS model 370 servo hydraulic fatigue machine with a 100 kN capacity. According to ASTM E 647 [3] the constant-force-amplitude procedure was used with a constant force range ΔP = 10.8 kN, (P_{min} = 1.20 kN and P_{max} = 12 kN) fixed stress ratio ($R = 0.1$) and loading frequency f = 13 Hz.

Thermographic sequences were acquired with constant intervals of 2000 cycles by using a cooled FLIR IR X6540 SC infrared camera with an InSb detector (640 × 512 pixels) and acquisition rate of 123 Hz, Fig. 4. A geometrical resolution of 0.067 mm/pixel was obtained placing the thermocamera at 170 mm from the specimen and by using a 50 mm lens with a 12 mm extension ring. All specimens were pre-cracked until to reaching a crack length of 2.5 mm according to ASTM E-647.

A second infrared camera, Deltatherm 1560 by Stress Photonics, with an InSb photonic detector (320 × 256 pixels) on the opposite side of the specimen was used only to monitoring the crack size according to Standard [3].

4. Methods and data analysis

In the Section 3, it has been shown as the heat dissipation increases two time for cycle with a typical trend in the case of adiabatic conditions ($Q = 0$). In order to estimate the heat dissipated, it is necessary to detect the surface temperature of the specimen during the test. The temperature variations of the material associated to the E_d will be hereafter indicated as T_d while the total temperature variation in one cycle as ΔT_d (Fig. 2b)).

In this way, the energy dissipated per cycle and in a unit of volume of material E_d is:

$$E_d = \rho c_p \Delta T_d \tag{3}$$

where ρ is the density and c_p is the specific heat at constant pressure of the material.

Since the linear increasing of energy is found two time per cycle, in the material, the temperature variation due to irreversible processes of fatigue damage will occur at twice the mechanical loading frequency [41], [43]. Eq. (3) is valid in both plane stress/strain conditions.

Fig. 5 shows the temperature variations due to the heat dissipated during a loading cycle in the case of the heat exchange by conduction, convection and radiation are null ($Q = 0$). It is easy to prove as the T_d trend can be decomposed as:

- an offset temperature (T_0), supposed to be constant in a loading cycle and in general, this assumption is valid for all the duration of the test at fixed loading level. T_0 represents the temperature of the body when the cycle starts,

Table 1
Chemical composition of AISI 422.

Materials [%]	C	P	Si	Ni	V	Mn	Cr	S	Mo	W
AISI 422	0.20–0.25	0.025	0.4	0.50–1.00	0.15–0.30	1.0	11.0–13.0	0.025	0.75–1.25	0.75–1.25

Table 2
Mechanical properties (at room temperature) of AISI 422.

Materials	E [MPa]	σ_y [MPa]	σ_{UTS} [MPa]
AISI 422	206000	760	966

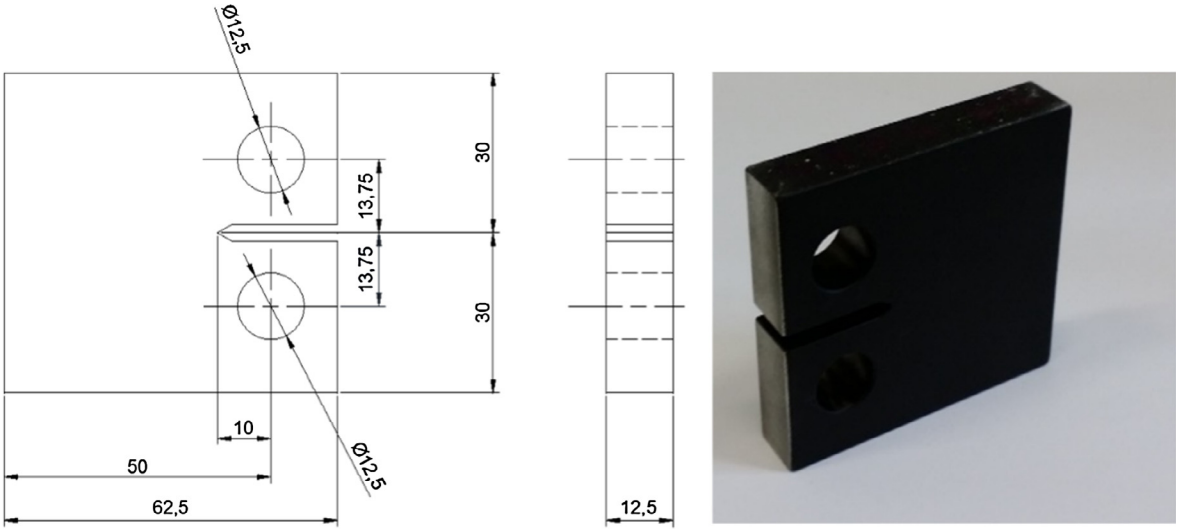

Fig. 3. Specimen dimension in mm according to ASTM E 647.

Fig. 4. Experimental set-up used for testing.

- a linear temperature increasing, with slope b over the number of cycles,
- a periodic temperature variation with amplitude $T_{2\omega}$ and period equal to (1/2)N.

Considering the Fig. 6, it can be seen as the total temperature variation ΔT_d and the temperature amplitude $T_{2\omega}$ are related through the angle γ:

$$\gamma = arctg\left(T_{2\omega}/\frac{N}{4}\right) = arctg(\Delta T_d/N) \tag{4}$$

and then:

$$4T_{2\omega} = \Delta T_d \tag{5}$$

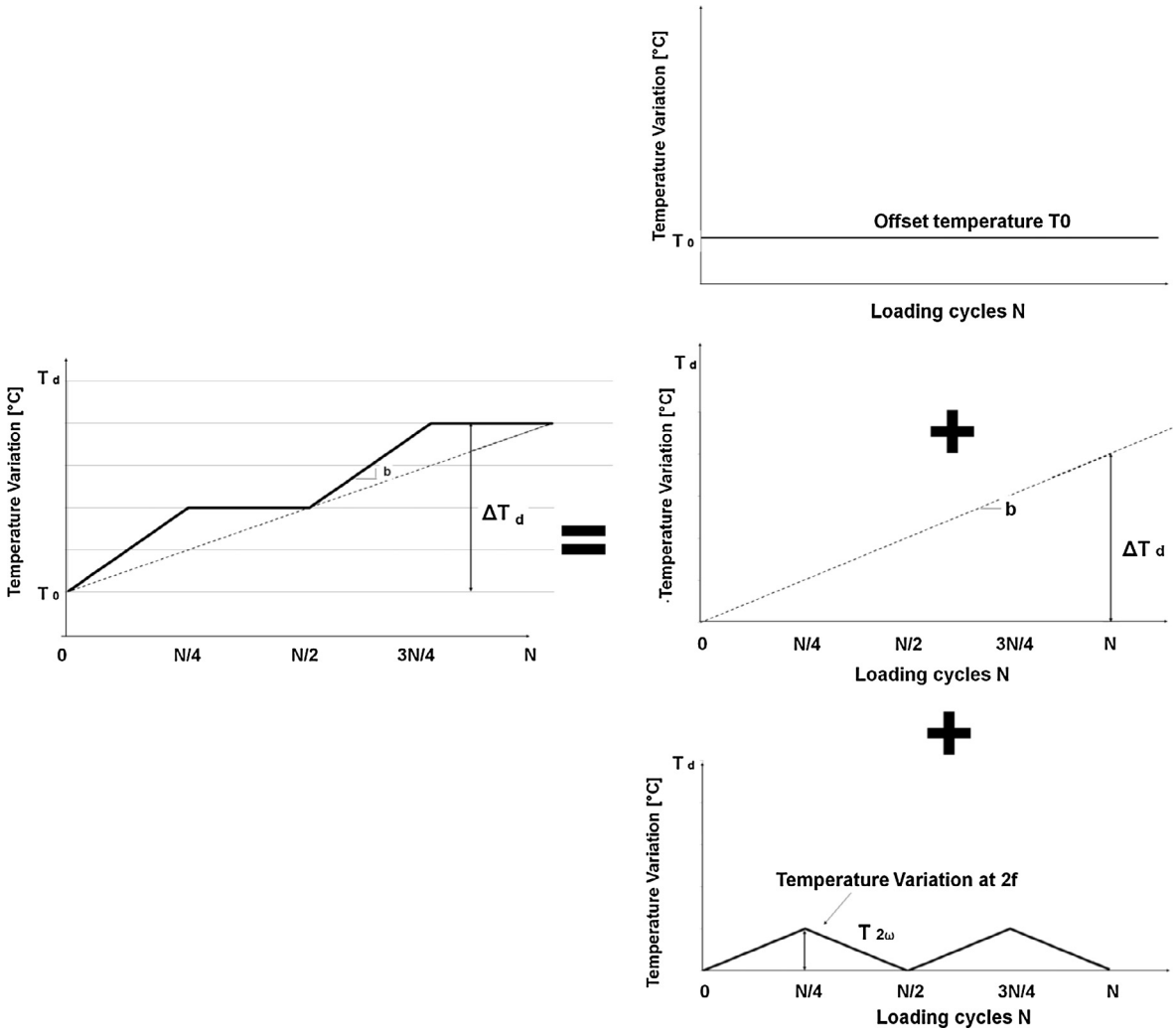

Fig. 5. Temperature variations due to the heat dissipated during a loading cycle in the case adiabatic conditions.

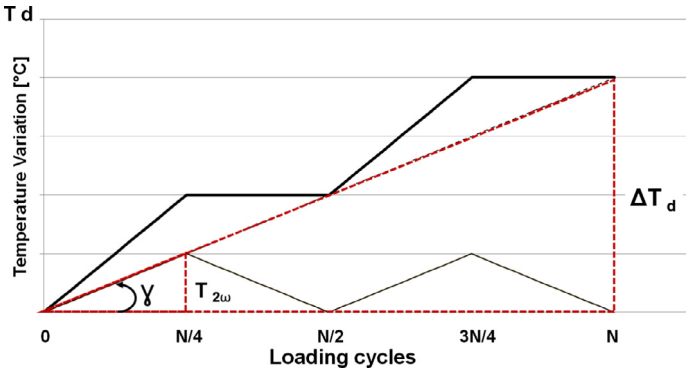

Fig. 6. Geometrical relation between the total temperature variation (ΔT_d) and the temperature amplitude at the twice of the loading frequency ($T_{2\omega}$).

$T2\omega$ can be obtained by assuming that the relative thermal signal component is a triangular function pulsating at $\omega_0 = 2\omega = 2(2\pi f)$ and it can be expanded as sum of cosine function terms:

$$T(t) = \frac{T_{2\omega}}{2} - A\sum_{1}^{\infty} \frac{1}{(2n+1)^2} \cos(2n-1)\omega_0 t \tag{6}$$

with

$$A = \frac{4T_{2\omega}}{9\pi^2} \tag{7}$$

Excluding high order components, for $n = 1$:

$$T(t) = \frac{T_{2\omega}}{2} - A\cos(2\omega t) \tag{8}$$

The last equation shows as the amplitude of the cosine term is directly related to ΔT_d. In other words, it is possible to obtain ΔT_d, by measuring the thermal signal component that occurs at twice the mechanical frequency, $T_{2\omega}$.

$$\Delta T_d = 4T_{2\omega} = 4\left(\frac{9\pi^2}{4}A\right) = 9\pi^2 A \tag{9}$$

By summarizing, the term E_d can be evaluated by knowing the slope b or the amplitude $T_{2\omega}$. In this regard, temperature signal can be studied in the time domain by the following model:

$$T(t) = T_0 + bt + A\cos(2\omega t + \phi_{2\omega}) \tag{10}$$

or rewriting in term of number of cycle:

$$T(N) = T_0 + \frac{b}{f}N + A\cos\left(2\omega\left(\frac{N}{f}\right) + \phi_{2\omega}\right) \tag{11}$$

where f is the loading frequency.

Adiabatic conditions are not easily guaranteed due to temperature gradient that arise during cyclic loading so, the real condition should consider that $Q \neq 0$ (heat exchanges cannot be neglected). In this case Eq. (9) is not valid anymore but, through the A term, a consistent E_d estimation can still be obtained since it is related to $T_{2\omega}$ which in turn, produces ΔT_d.

In this work, the Eq. (10) has been used to extract the A term in order to obtain, pixel by pixel, the temperature variations ΔT_d per cycle and then the estimation E_d term. As just said, this term represents the energy dissipated as heat in a unit of volume and for cycles so, the total heat dissipated (J/cycles) can be expressed as:

$$Q_d = E_d V_p \tag{12}$$

where V_p is the plastic volume at the crack tip that can be estimated following Irwin [44] in plane stress conditions:

$$V_p = r_p B = \frac{1}{2\pi}\left(\frac{\Delta K}{\sigma_y}\right)^2 B \tag{13}$$

and B is the specimen thickness. The model adopted for evaluating V_p refers to plane stress conditions. The shape and size of the plastic volume change through the thickness due to the plane strain conditions in the centre of the specimen which produces a little overestimation of V_p and then Q_d. Nevertheless, as will be demonstrated furtherly, by experimental data, this does not prejudice the quality of results.

In the next section, the procedure above described will be used to process thermographic data acquired during the fatigue test at time intervals of 2000 cycles. Then, Eq. (12) will be used in order to assess the heat dissipated at the crack tip.

5. Results and discussion

As described in previous sections, thermographic sequences were acquired during constant load intervals of 2000 cycles and coefficients T_0, b and A were assessed through Eq. (10). The first two are related to the temperature rise ahead the crack tip due to the heat dissipated in the plastic volume. As already said, this heat can become difficult to assess due to heat exchanges for conduction, convection and radiation. The term A is more strictly related to dissipated energy.

Fig. 7 shows T_0 maps in correspondence of three different values of number of cycles (specimen 1). It is evident that a significant rise of temperature is only visible in proximity of failure and for high values of ΔK_I. This result is due to the prevalence of heat exchanges with respect to the heat dissipated related to plastic phenomena, as it was also pointed out in the work of Meneghetti et al. [26]. In the same figure, on the contrary, it can be seen that the thermal signal component that occurs at twice the mechanical frequency presents significant values from the first loading cycles. This is more evident in Fig. 8, where it is possible to identify two zones (A1 and A2) characterized by a significant rise of the signal by considering the signal trend along the crack growth direction. This particular trend is due to two different effects: the crack closure effect [45] (A1) and the plastic conditions ahead of the crack tip (A2). In fact, as already described in literature [45], the crack closure can be induced by the plasticity at the crack tip, the contact of the fracture surfaces caused by the misfit of the microscopically rough fracture surfaces and the asperity contacts. The two different effects are also clearly described in the phase maps since they determine a change of phase with opposite sign in respect to the sound area (Fig. 7). It is worth to notice that the two zones A1 and A2 are clearly visible but the effect of the crack closure decrease with the increase of the crack length and SIF being this effect more and more negligible for high values of crack length and SIF.

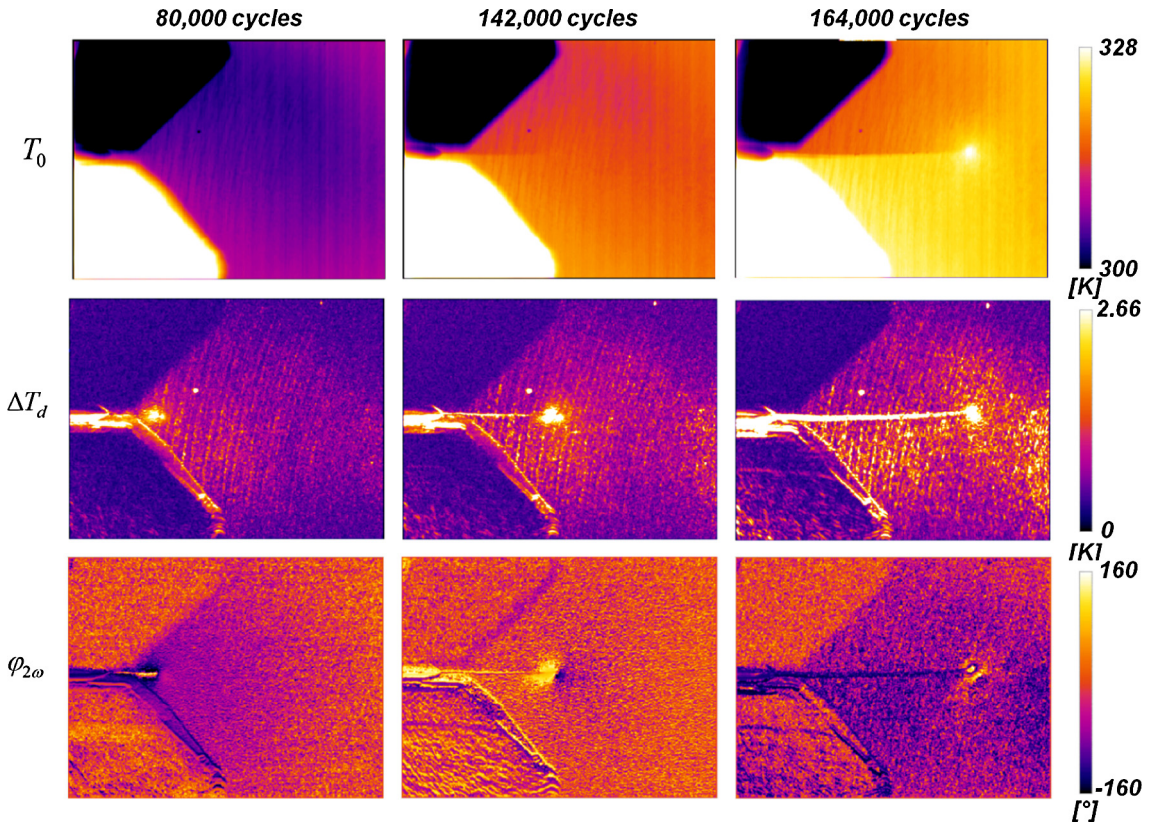

Fig. 7. Maps of the absolute temperature T_0, the total temperature due to the heat dissipated (ΔT_d) and the phase signal of the temperature at twice of the loading frequency ($\phi_{2\omega}$), obtained in correspondence of three number of cycles (specimen 1).

In Fig. 8, it is reported the phase signal $\phi_{2\omega}$ that occurs at twice the mechanical frequency along the same profile used for assessing the behaviour of temperature signal. The phase changes in sign by passing through the A2 to the A1 zone and reaches the zero value in correspondence the relative minimum value of the ΔT_d between A2 and A1. This point represents the crack tip position and in this regard, the phase signal at the twice of loading frequency could be used for evaluating the crack growth in similar way to the thermoelastic phase signal [38]. However, this topic is out of aims of this work and it will be better investigated in further works.

In Fig. 9 there are reported $\Delta T_{d(\max)}$ values as function of the number of cycles (specimen 1). These values represent the maximum values of ΔT_d reached in the plastic zone (A2 area). As expected, the $\Delta T_{d(\max)}$ values increase as the number of cycles increase in similar way at the crack growth rate.

Eqs. (3), (12) and (13) were used to assess the heat dissipated for cycle (Q_d) considering in Eq. (3) the $\Delta T_{d(\max)}$ values.

In Fig. 10, the heat dissipated at the crack tip is reported versus the stress intensity factor (SIF) values for each specimen. It is very interesting to observe that the heat dissipated depends on the fourth power of the SIF. In this way, the relation between Q_d and ΔK can be generally expressed by the following relation:

$$Q_d = n\Delta K^4 \tag{14}$$

with n equal to a constant value.

Eq. (14) is in agreement with the equation obtained by Weertman [19] to describe the fatigue crack growth through an energy based approach:

$$da/dN = A_1 \Delta K^4/(\mu \sigma_c^2 U_c) \tag{15}$$

where da/dN is the crack growth rate, μ, the shear modulus of the material, σ_c, the critical stress at fracture, and A_1, a constant. U_c is defined as the critical energy to create a unit surface:

$$U_c = Q_{HE}/(2bda/dN) \tag{16}$$

where, Q_{HS} is the hysteresis energy and b is the specimen thickness.

Fig. 11(a), shows the evolution of the crack growth rate with respect to the heat dissipated per cycle considering the data obtained with specimens 2 and 3. Also in this case, a linear relation can be determined between these two parameters:

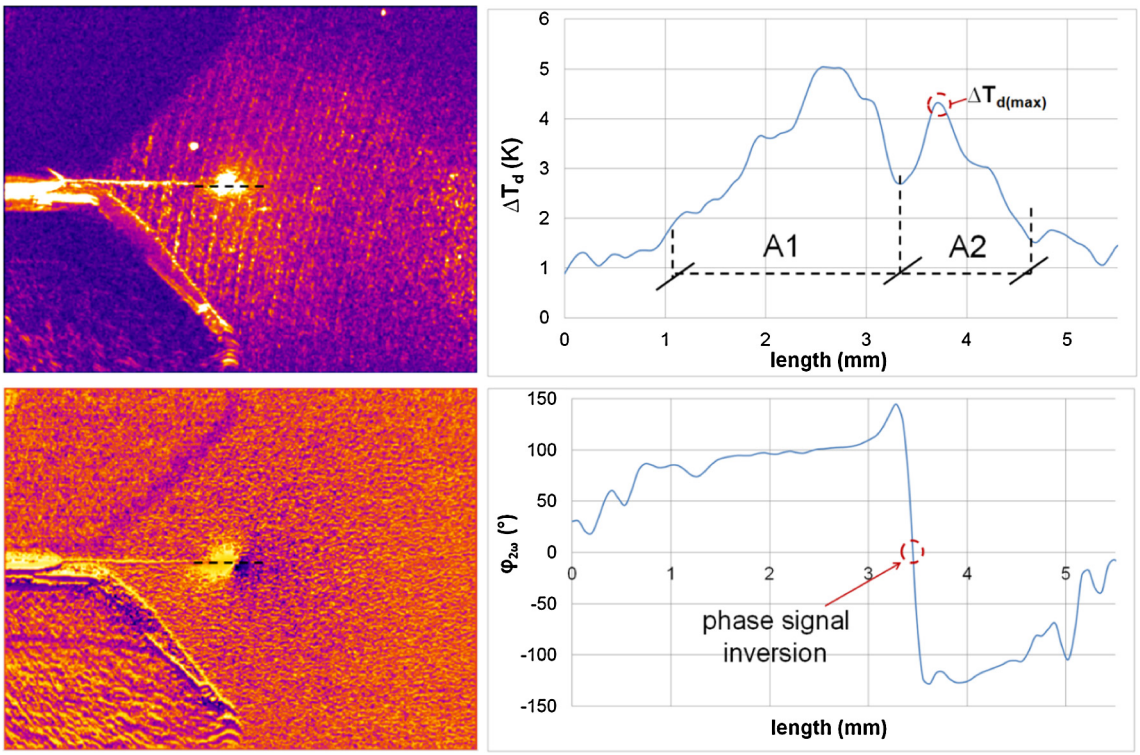

Fig. 8. Total temperature and phase maps (142,000 cycles) and total temperature and phase profiles along the crack growth direction.

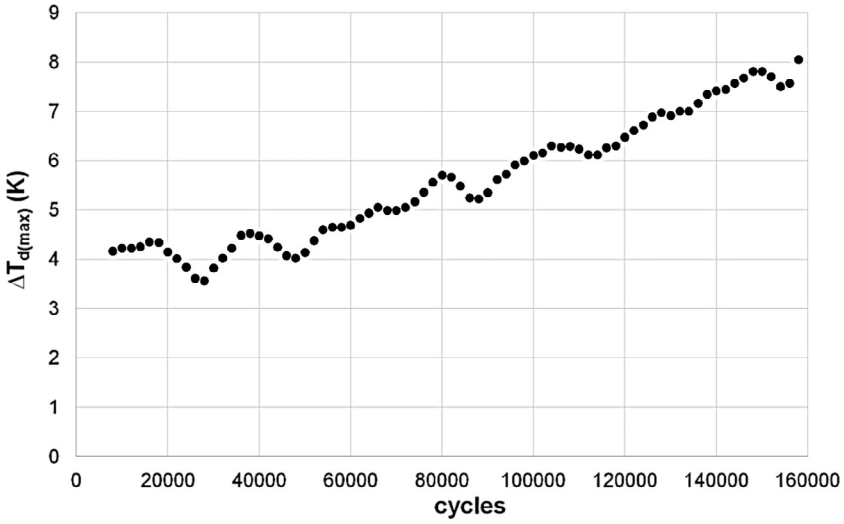

Fig. 9. $\Delta T_{d(\max)}$ values as function of the number of cycles for specimen 1.

$$\frac{da}{dN} = C_1 Q_d^{C_2} \tag{17}$$

A similar relation has been determined and verified by other authors by considering the dissipated hysteretic energy per cycle in place of the heat dissipated [22].

Eq. (17) can be used to assess the crack growth rate by knowing the heat dissipated per cycle ahead of the crack tip. To do that, in this work, the thermographic data of the specimens 2 and 3 have been used for evaluating the coefficients C_1 and C_2 then, the linear model has been used for predicting the crack growth rate of the specimens 1.

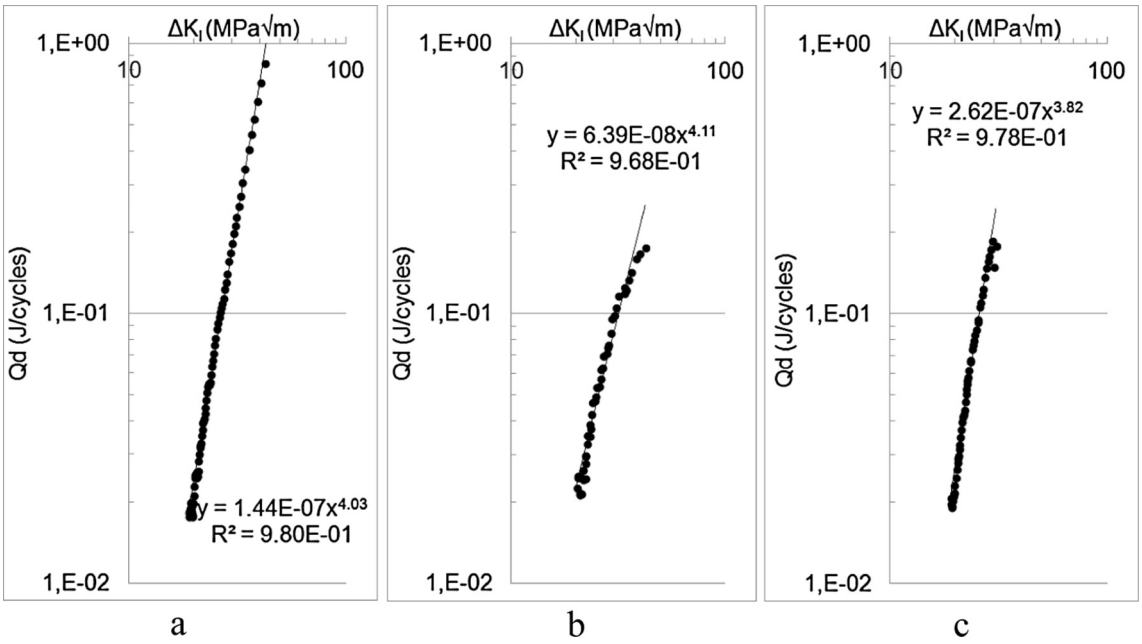

Fig. 10. Estimated heat dissipated energy per cycle as function of the ΔK_I, (a) specimen 1, (b) specimen 2, (c) specimen 3.

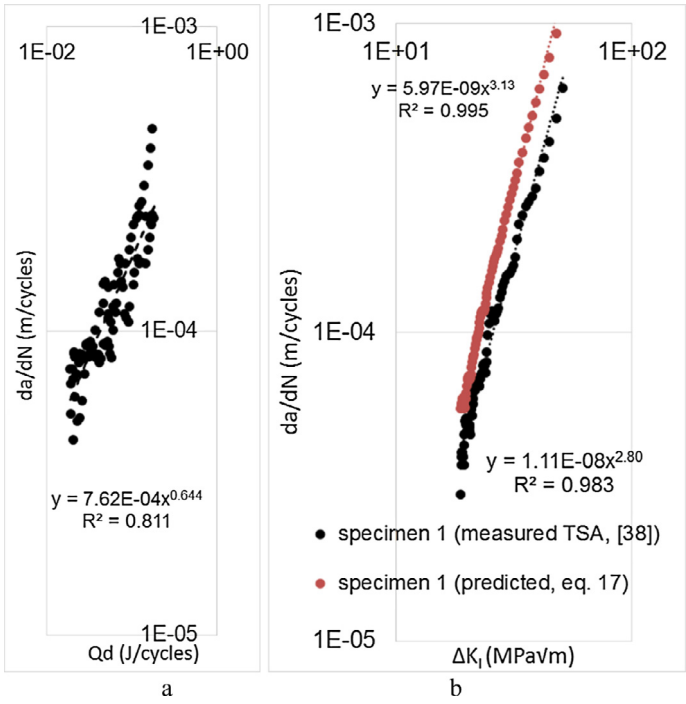

Fig. 11. (a) Crack growth rate as function of the estimated heat dissipated energy per cycle and (b) comparison of predicted values obtained with the proposed procedure and measured values in [38].

In Fig. 11(b) are shown the results obtained by applying the Eq. (17) and the comparison with the crack growth rate measured by means of TSA [38]. In particular, in [38], the phase of thermoelastic signal has been used to estimate the crack tip position over time. This procedure, as already said, has been used by other authors [11–18] and validated by comparison with optical measurements [12].

It is worth to notice that the so called "predicted" and "measured" values have been obtained by using the same experimental set-up.

The SIF values were evaluated according to the Standard ASTM E 647 [3] and the following equation:

$$\Delta K = \frac{\Delta P}{B\sqrt{W}} \frac{(2+\beta)}{(1-\beta)^{3/2}} (0.886 + 4.64\beta - 13.32\beta^2 + 14.72\beta^3 - 5.6\beta^4) \tag{18}$$

where $\beta = a/W$, a is the crack length, B and W are two characteristic dimensions of specimen [3], in this case $B = 12.5\ mm$ and $W = 50\ mm$.

It can be seen in Fig. 11(b) as the predicted values are in good agreement with measured ones. It is worth to highlight as the accuracy of the obtained results can be improved by increasing the number of data since data obtained only by two specimens (2 and 3) have been used to obtain the coefficients of the Eq. (17). Moreover, the scatter between the predicted and measured data can be due to the error in Q_p calculations (due to the oversized V_p).

6. Conclusions

In this work, a new procedure based on the processing of thermographic data has been proposed for evaluating the crack growth rate through the assessment of heat dissipated at the crack tip during fracture mechanics tests continuously.

Three CT specimens of the martensitic stainless steel AISI 422 were tested and monitored by means of a cooled infrared camera in order to acquire thermographic sequences during tests at regular intervals (2000 cycles each).

The proposed procedure uses the analysis of the thermal signal in the frequency domain in order to extract the thermal component related to the heat dissipated at the crack tip. This latter, in the plastic zone varies at the twice of the loading frequency and can be used for estimating the heat dissipated for cycle.

It was demonstrated as the estimated heat dissipated evaluated with thermographic approach can be used for predicting the fatigue crack growth after a previous calibration procedure (energetic approach). Moreover, with respect to traditional experimental techniques, the proposed approach allows for the on-line monitoring of the crack growth automatically.

Others interesting results can be summarized as follows:

- the temperature rise in the plastic zone is only visible in proximity of failure and for high values of ΔK_I,
- the thermal signal component that occurs at twice the mechanical frequency presents significant values in the plastic zone from the first loading cycles and allows for evaluating also the crack closure effect,
- a similar Paris Law model was obtained between the crack growth and the heat dissipated per cycle,
- it was obtained a fourth power dependence of heat dissipated energy and Stress Intensity Factor in agreement with numerical and analytical models present in literature.

Finally, it is worth to underline as the proposed method can also be used for the monitoring of damage or crack growth within real and more complex structures subjected to actual loading conditions.

Acknowledgements

This work is part of a large-scale research project (PON-SMATI) aimed at identifying innovative steels to turbo machinery used in extreme environmental conditions. The authors would like to thank GE oil & gas (Nuovo Pignone S.r.l.) for the support and collaboration provided in the experimental tests.

References

[1] Paris P, Erdogan F. A critical analysis of crack propagation laws. J Basic Eng, Trans Am Soc Mech Engineers, 1963; D 85(4): 528–7, http://dx.doi.org/10.1115/1.3656900.
[2] Ritchie RO. Mechanisms of fatigue-crack propagation in ductile and brittle solids. Int J Fract 1999; 100:55-29.
[3] ASTM E 647–00: Standard Test Method for Measurement of Fatigue Crack Growth Rates, 2004.
[4] Réthore J, Limodin N, Buffière JY, Roux S, Hild F. Three-dimensional analysis of fatigue crack propagation using X-Ray tomography, digital volume correlation and extended finite element simulations. Proc IUTAM 2012;4(4):151–8.
[5] Tanabe H, Kida K, Takamatsu T, Itoh N, Santos EC. Observation of Magnetic Flux Density Distribution around Fatigue Crack and Application to Non-Destructive Evaluation of Stress Intensity Factor. Proc Eng 2011;10:881–7.
[6] Yates JR, Zanganeh M, Tai YH. Quantifying crack tip displacement fields with DIC. Eng Fract Mech 2010;77:2063–76.
[7] Guduru PR, Zehnder AT, Rosakis AJ, Ravichandran G. Dynamic full field measurements of crack tip temperatures. Eng Fract Mech 2001;68:1535–56.
[8] Carrascal I, Casado JA, Diego S, Lacalle R, Cicero S, Álvarez JA. Determination of the Paris' law constants by means of infrared thermographic techniques. Polym Testing 2014;40. 39-7.
[9] Cui ZQ, Yang HW, Wang WX, Yan ZF, Ma ZZ, Xu BS, et al. Research on fatigue crack growth beahavior of AZ31B magnesium alloy electron beam welded joints based on temperature distribution around the crack tip. Eng Fract Mech 2015;133. 14-10.
[10] Fedorova AYU, Bannikov MV, Plekhov OA, Plekhova EV. Infrared thermography study of the fatigue crack propagation. Frattura ed Integrità Strutturale 2012;21:46–8.
[11] Tomlinson RA, Olden EJ. Thermoelasticity for the analysis of crack tip stress fields – a review. Strain 1999;35. 49-7.
[12] Tomlinson RA, Patterson EA. Examination of crack tip plasticity using thermoelastic stress analysis. Thermomech Infra-Red Imaging. In: Proceedings of the society for experimental mechanics series 2011; vol. 7, p. 123–7.

[13] Diaz FA, Patterson EA, Tomlinson RA, Yates RA. Measuring stress intensity factors during fatigue crack growth using thermoelasticity. Fract Eng Mater Struct 2004;27(7). 571–13.
[14] Diaz FA, Patterson EA, Yates RA. Some improvements in the analysis of fatigue cracks using thermoelasticity. Int J Fatigue 2004;26(4). 365–12.
[15] Diaz FA, Patterson EA, Yates RA. Application of thermoelastic stress analysis for the experimental evaluation of the effective stress intensity factor. Frattura ed Integrità Strutturale 2013;25. 109-8.
[16] Diaz FA, Patterson EA, Yates RA. Differential Thermography Reveals Crack Tip Behaviour? In: Proc 2005 SEM Annual Conf on Exp App Mech, Society for Experimental Mechanics, 2005; p. 1413–6.
[17] Ancona F, De Finis R, Palumbo D, Galietti U. Crack growth monitoring in stainless steels by means of TSA technique. Proc Eng 2015;109. 89-8.
[18] Palumbo D, Ancona F, De Finis R, Galietti U. Experimental study of the crack growth in stainless steels using thermal methods. Proc Eng 2015;109. 338-8.
[19] Weertman J. Theory of fatigue crack growth based on a BCS crack theory with work hardening. Int J Fatigue 1973;9:125–31.
[20] Klingbeil NW. A total dissipated energy theory of fatigue crack growth in ductile solids. Int J Fatigue 2003. 117-12.
[21] Mazari M, Bouchouicha B, Zemri M, Benguediab M, Ranganathan N. Comput Mater Sci 2008;41:344–6.
[22] Kucharski P, Lesiuk G, Szata M. Description of fatigue crack growth in steel structural components using energy approach – influence of the microstructure on the FCGR. In: Fatigue failure and fracture mechanics XXVI: proceedings of the XXVI Polish National Conference on Fatigue Failure and Fracture Mechanics, (Dariusz Skibicki, ed.), AIP Publishing, 2016.
[23] Ranganathan N, Chalon F, Meo S. Some aspects of the energy based approach to fatigue crack propagation. Int J Fatigue 2008;30:1921–8.
[24] Ikeda S, Izumi Y, Fine ME. Plastic work during fatigue crack propagation in a high strength low alloy steel and in 7050 Al alloy. Eng Fract Mech 1977;9:123–6.
[25] Gross TS, Weertman J. Calorimetric measurement of the plastic work of fatigue crack propagation in 4140 steel. Metall Trans A 1982;13A:2165–72.
[26] Meneghetti G, Ricotta M. Evaluating the heat energy dissipated in a small volume surrounding the tip of a fatigue crack 2016;92(2):605–11.
[27] Palumbo D, Galietti U. Characterization of steel welded joints by infrared thermographic methods. Quant Infrared Thermography J 2014;11. 42-11.
[28] Galietti U, Palumbo D. Application of thermal methods for characterization of steel welded joints. In: 14th international conference on experimental mechanics, ICEM 2014; Poitiers; France; 4–9 July 2010. EPJ Web of Conferences, vol. 6, Article number 38012.
[29] Palumbo D, Galietti U. Thermoelastic Phase Analysis (TPA): a new method for fatigue behaviour analysis of steels. Fatigue Fract Eng Mater Struct 2017;4. 523-12.
[30] Dulieu-Barton JM. Introduction to thermoelastic stress analysis. Strain 1999;35. 35-5.
[31] Pitarresi G, Patterson EA. A review of the general theory of thermoelastic stress analysis. J Strain Anal Eng Des 2003;38(5):405–13.
[32] Wang WJ, Dulieu-Barton JM, Li Q. Assessment of non-adiabatic behaviour in thermoelastic stress analysis of small scale components. Exp Mech 2010;50. 449-13.
[33] Harwood N, Cummings WM. Thermoelastic stress analysis. Bristol Philadelphia and New York: Adam Hilger; 1991.
[34] Palumbo D, Galietti U. Data correction for thermoelastic stress analysis on titanium components. Exp Mech 2016;56(3). 451-12.
[35] Stanley P. Applications and potential of thermoelastic stress analysis. J Mater Process Technol 1997;64. 359-12.
[36] Dunn SA. Using nonlinearities for improved stress analysis by thermoelastic techniques. Appl Mech Rev 1997;50(9). 499-15.
[37] Dulieu-Smith SM. Alternative calibration techniques for quantitative thermoelastic stress analysis. Strain 1995;31. 9-8.
[38] Ancona F, Palumbo D, De Finis R, Demelio GP, Galietti U. Automatic procedure for evaluating the Paris Law of martensitic and austenitic stainless steels by means of thermal methods. Eng Fract Mech 2016;163:206–14.
[39] Meneghetti G. Analysis of the fatigue strength of a stainless steel based on the energy dissipation. Int J Fatigue 2007;29. 81-14.
[40] Wang C, Blanche A, Wagner D, Chrysochoos A, Bathias C. Dissipative and microstructural effects associated with fatigue crack initiation on an Armco iron. Int J Fatigue 2014;58:152–7.
[41] Enke NF, Sandor BL. Cyclic plasticity analysis by differential infrared thermography. In: Proceeding of the VI International Congress on experimental Mechanics, June, 7, 1988; p. 830–35.
[42] Tomei R. Criteri di scelta degli acciai inossidabili in funzione degli impieghi. La meccanica italiana. 1981; 147.
[43] De Finis R, Palumbo D, Galietti U. Mechanical behaviour of Stainless Steels under Dynamic Loading: An Investigation with Thermal Methods. J Imaging 2016;2(4):32.
[44] Irwin GR. Linear fracture mechanics, fracture transition and fracture control. Eng Fract Mech 1968;1:241–57.
[45] Pippan R, Hohenwarter A. Fatigue crack closure: a review of the physical phenomena. Fatigue Fract Eng Mater Struct 2017;40(4). 471-25.